



Research article

On the stochastic modeling and forecasting of the $SVIR$ epidemic dynamic model under environmental white noise

Shah Hussain¹, Naveed Iqbal¹, Elissa Nadia Madi², Mohsen Bakouri^{3,4}, Ilyas Khan^{5,6,*} and Wei Sin Koh⁷

¹ Department of Mathematics, College of Science, University of Ha'il, Ha'il 2440, Saudi Arabia

² Faculty of Informatics and Computing, Universiti Sultan Zainal Abidin (UniSZA), Besut Campus, Terengganu, Malaysia

³ Department of Medical Equipment Technology, College of Applied Medical Science, Majmaah University, Al Majmaah 11952, Saudi Arabia

⁴ Department of Physics, College of Arts, Fezzan University, Traghen 71340, Libya

⁵ Department of Mathematics, College of Science, Al-Zulfi, Majmaah University, Al Majmaah 11952, Saudi Arabia

⁶ Hourani Center for Applied Scientific Research, Al-Ahliyya Amman University, Amman, Jordan

⁷ INTI International University, Persiaran Perdana BBN Putra Nilai, 71800 Nilai, Negeri Sembilan, Malaysia

* **Correspondence:** Email: i.said@mu.edu.sa.

Abstract: This study introduced a novel $SVIR$ epidemic model incorporating environmental white noise to account for stochastic fluctuations in disease transmission. The model was analyzed to determine conditions for disease persistence and extinction, with outcomes linked to the basic reproduction number. A numerical approach was employed to facilitate computational analysis, and simulations were conducted using data from existing literature to generate realistic predictions. The stochastic model was further evaluated against its deterministic counterpart to assess predictive accuracy. The results highlight the significant role of randomness in epidemiological dynamics, providing valuable insights into disease spread and control strategies.

Keywords: infectious disease; stochastic model; persistence; existence; simulation

Mathematics Subject Classification: 26A33, 34A08, 35R11

1. Introduction

The study of epidemic models has gained increasing importance due to the rising frequency and impact of infectious diseases on global health. These models provide essential frameworks for understanding disease spread and devising effective control strategies. Among these, the susceptible-vaccinated-infectious-recovered ($\mathcal{S}\mathcal{V}\mathcal{I}\mathcal{R}$) model plays a crucial role in analyzing diseases where vaccination is a key factor in mitigating outbreaks.

Traditional deterministic epidemic models assume homogeneous populations and predictable disease spread. However, real-world epidemics exhibit significant randomness due to environmental fluctuations, human behavior, and uncertainties in vaccination coverage. To address these complexities, researchers have incorporated stochasticity into epidemic models, leading to more realistic predictions. Recent advancements in stochastic $\mathcal{S}\mathcal{V}\mathcal{I}\mathcal{R}$ models have explored various aspects, including optimal vaccination strategies, the influence of media on disease spread, and the impact of different types of noise [1–3].

In this work, we focus on a stochastic $\mathcal{S}\mathcal{V}\mathcal{I}\mathcal{R}$ model that accounts for non-constant population sizes and random fluctuations in transmission and vaccination rates. By integrating stochastic elements into key parameters, we aim to capture the inherent randomness of real-world epidemics. Our numerical analyses highlight how vaccination strategies can effectively control disease spread, even under unpredictable disturbances. These findings contribute to understanding the interplay between stochastic influences, vaccination, and population dynamics, offering valuable insights for epidemic control and management [4].

Building upon previous research, including the foundational works of Allen [5], Brauer [6], Gray et al., Rozhnova et al., and Witbooi [7–9], we examine how noise and other stochastic factors affect the long-term behavior of $\mathcal{S}\mathcal{V}\mathcal{I}\mathcal{R}$ models.

This study addresses these gaps by developing a stochastic $\mathcal{S}\mathcal{V}\mathcal{I}\mathcal{R}$ model that incorporates environmental white noise, capturing the inherent variability in epidemic dynamics. Unlike previous studies, the model explicitly accounts for random fluctuations in both disease transmission and vaccination rates while considering a dynamic population size. This approach provides a more comprehensive framework to evaluate the interplay between stochasticity, vaccination strategies, and population dynamics, ultimately advancing the field of stochastic epidemic modeling.

This study builds on the work of Joko Harianto and Titik Suparwati, who initially developed an $\mathcal{S}\mathcal{V}\mathcal{I}\mathcal{R}$ model to assess the effectiveness of various vaccination strategies [10]. They structured the model into four distinct compartments: \mathcal{S}_t for susceptible individuals, \mathcal{V}_t for vaccinated individuals, \mathcal{I}_t for infected individuals, and \mathcal{R}_t for recovered individuals.

In our model, we define β as the transmission rate necessary for disease spread and assume a constant recovery rate denoted by γ . The rate at which susceptible individuals are vaccinated is represented by α , while disease-induced mortality is captured by ω . The natural mortality rates, which are unrelated to the disease, are given as μ_1 for the susceptible group, μ_2 for the vaccinated, μ_3 for the infected, and μ_4 for the recovered individuals. Newborns are added to the susceptible class at a constant rate μ , ensuring a continuous supply of individuals who can potentially contract the disease.

Furthermore, γ_1 represents the rate at which susceptible individuals acquire immunity and transition into the recovered compartment. The model assumes that immunity gained through vaccination is long-lasting and equivalent to natural immunity. However, vaccinated individuals may still be susceptible to

infection, albeit at a reduced rate β_1 , reflecting partial immunity or lower effective contact with infected individuals. This comprehensive model is formulated as follows [10]:

$$\frac{d}{dt} \begin{pmatrix} \mathcal{S} \\ \mathcal{V} \\ \mathcal{I} \\ \mathcal{R} \end{pmatrix} = \begin{pmatrix} \mu - \mathcal{S}(\mu_1 + \beta\mathcal{I} + \alpha) \\ \alpha\mathcal{S} - \mathcal{V}(\beta_1\mathcal{I} + \gamma_1 + \mu_2) \\ \mathcal{I}(\beta\mathcal{S} + \beta_1\mathcal{V}) - \mathcal{I}(\gamma + \mu_3 + \omega) \\ \gamma_1\mathcal{V} + \gamma\mathcal{I} - \mu_4\mathcal{R} \end{pmatrix}. \quad (1.1)$$

We begin our analysis with the following initial conditions: $\mathcal{S}_0 > 0$, $\mathcal{V}_0 > 0$, $\mathcal{I}_0 > 0$, and $\mathcal{R}_0 > 0$. These initial values represent the population sizes for the susceptible, vaccinated, infected, and recovered groups, respectively, at the initial time point $t = 0$, reflecting the population's status at the start of the observational period.

Importantly, the initial population satisfies the relation:

$$\mathcal{S}_0 + \mathcal{V}_0 + \mathcal{I}_0 + \mathcal{R}_0 = \mathcal{N}, \quad (1.2)$$

where \mathcal{N} represents the total population size, ensuring that all individuals in the population are accounted for. In the deterministic $\mathcal{S}\mathcal{V}\mathcal{I}\mathcal{R}$ model, the total population remains constant as births and deaths balance out. However, in the stochastic version, the total population may decrease over time due to the influence of stochastic perturbations.

To maintain biological plausibility and consistency, all model parameters are assumed to be strictly positive. This assumption prevents biologically unrealistic values and ensures the system remains well-defined.

Following the theoretical framework outlined in [10], the system exhibits key properties that govern disease transmission dynamics over time. While the total population remains constant in the deterministic setting, the distribution of individuals among the compartments evolves dynamically based on the model's parameters.

By ensuring that all parameters are strictly positive and that the population distribution is comprehensive, the model remains consistent with real-world epidemiological scenarios. This approach allows for an accurate representation of disease spread and the impact of intervention strategies.

- The disease-free equilibrium, denoted as $\mathcal{E}_0 = (\mathcal{S}_0, \mathcal{V}_0, \mathcal{I}_0, \mathcal{R}_0)$, is given by:

$$\mathcal{E}_0 = \left(\frac{\mu}{\alpha + \mu_1}, \frac{\alpha\mu}{(\alpha + \mu_1)(\gamma_1 + \mu_2)}, 0, \frac{\gamma_1\alpha\mu}{\mu_4(\alpha + \mu_1)(\gamma_1 + \mu_2)} \right).$$

This equilibrium exists and is globally asymptotically stable if the basic reproduction number \mathfrak{R}_0 satisfies the condition:

$$\mathfrak{R}_0 = \frac{\beta\mu}{(\alpha + \mu_1)(\mu_3 + \gamma + \omega)} + \frac{\beta_1\alpha\mu}{(\alpha + \mu_1)(\mu_3 + \gamma + \omega)(\gamma_1 + \mu_2)} \leq 1.$$

- If the basic reproduction number \mathfrak{R}_0 is less than or equal to one ($\mathfrak{R}_0 \leq 1$), the system stabilizes at a disease-free equilibrium. In this case, the infection cannot sustain itself within the population and eventually dies out. When $\mathfrak{R}_0 \leq 1$, any initial outbreak will dissipate over time as the number of infected individuals declines to zero.

Conversely, if \mathfrak{R}_0 exceeds one ($\mathfrak{R}_0 > 1$), the system's dynamics change significantly. The model then predicts the existence of an endemic equilibrium, where the disease persists in the population at a stable level. This means that the infection will not be eradicated but will remain within the population over time. The infected compartment, represented by \mathcal{I} , will only maintain a non-zero value when the condition $\mathfrak{R}_0 > 1$ holds. Therefore, the establishment of an endemic state is directly linked to this threshold, mathematically represented as follows:

$$\begin{aligned} \mathcal{E}^+ &= (\mathcal{S}^+, \mathcal{V}^+, \mathcal{I}^+, \mathcal{R}^+) \\ &= \left(\frac{\mu}{\alpha + \mu_1 + \beta \mathcal{I}^+}, \frac{\alpha \mu}{(\alpha + \mu_1 + \beta \mathcal{I}^+)(\gamma_1 + \mu_2 + \beta_1 \mathcal{I}^+)}, \mathcal{I}^+, \frac{\gamma_1 \mathcal{V}^+ + \gamma \mathcal{I}^+}{\mu_4} \right) \end{aligned}$$

where \mathcal{I}^+ is the positive root of $\theta(\mathcal{I}) = \mathcal{O}_1 \mathcal{I}^2 + \mathcal{O}_2 \mathcal{I} + \mathcal{O}_3(1 - \mathfrak{R}_0)$, where:

- $\mathcal{O}_1 = (\mu_3 + \gamma + \omega)\beta_1\beta > 0$,
- $\mathcal{O}_2 = (\mu_3 + \gamma + \omega)[(\alpha + \mu_1)\beta_1 + (\gamma_1 + \mu_2)\beta] - \beta_1\beta\mu$,
- $\mathcal{O}_3 = (\mu_3 + \gamma + \omega)(\alpha + \mu)(\gamma_1 + \mu) > 0$.

Environmental factors significantly impact biomathematical models in real-world scenarios, as evidenced by recent studies [11, 12]. To accurately capture the dynamics of epidemics within such unpredictable environments, it is essential to employ stochastic differential equations. Recent literature has extensively explored epidemic models influenced by environmental white noise [13–15].

This paper aims to elucidate the effects of white noise on epidemic dynamics by analyzing a stochastic $\mathcal{S}\mathcal{V}\mathcal{I}\mathcal{R}$ model. We hypothesize that stochastic white noise directly influences the compartments \mathcal{S}_t , \mathcal{V}_t , \mathcal{I}_t , and \mathcal{R}_t , as explored in [16, 17]. Building on this perspective, we develop and analyze the following stochastic $\mathcal{S}\mathcal{V}\mathcal{I}\mathcal{R}$ model by introducing perturbations in the parameters α and γ .

While the deterministic model offers valuable insights, it does not capture the randomness inherent in real-world epidemic scenarios. To address this, we introduce stochastic elements into the transmission and vaccination processes by perturbing the parameters $\alpha \rightarrow \alpha + \sigma_1 d\mathcal{B}_1$ and $\gamma \rightarrow \gamma + \sigma_2 d\mathcal{B}_2$, resulting in:

$$\begin{aligned} d\mathcal{S} &= (\mu - \mu_1 \mathcal{S} - \beta \mathcal{S} \mathcal{I} - \alpha \mathcal{S})dt - \sigma_1 \mathcal{S} d\mathcal{B}_1, \\ d\mathcal{V} &= (\alpha \mathcal{S} - \beta_1 \mathcal{V} \mathcal{I} - \gamma_1 \mathcal{V} - \mu_2 \mathcal{V})dt + \sigma_1 \mathcal{S} d\mathcal{B}_1, \\ d\mathcal{I} &= (\beta \mathcal{S} \mathcal{I} + \beta_1 \mathcal{V} \mathcal{I} - \gamma \mathcal{I} - \mu_3 \mathcal{I} - \omega \mathcal{I})dt - \sigma_2 \mathcal{I} d\mathcal{B}_2, \\ d\mathcal{R} &= (\gamma_1 \mathcal{V} + \gamma \mathcal{I} - \mu_4 \mathcal{R})dt + \sigma_2 \mathcal{I} d\mathcal{B}_2. \end{aligned} \tag{1.3}$$

Within our stochastic $\mathcal{S}\mathcal{V}\mathcal{I}\mathcal{R}$ model, the terms $\mathcal{B}_1(t)$ and $\mathcal{B}_2(t)$ represent independent standard Brownian motion processes. These stochastic processes are essential components of the model, introducing randomness into the system and allowing us to simulate the unpredictable fluctuations that occur in real-world epidemic dynamics. The independence of $\mathcal{B}_1(t)$ and $\mathcal{B}_2(t)$ ensures that the random influences they represent do not correlate, thereby accurately capturing the inherent variability in both disease transmission and vaccination rates.

The coefficients σ_1^2 and σ_2^2 represent the variances of the stochastic perturbations associated with α and γ , respectively. Specifically, σ_1^2 corresponds to the variance of the noise affecting the vaccination

rate α , while σ_2^2 pertains to the variance of the noise influencing the recovery rate γ . These variances determine the intensity of the stochastic fluctuations: higher values imply a greater degree of randomness within the system.

Introducing stochastic perturbations into epidemiological models allows for a more nuanced representation of disease dynamics. These perturbations account for random environmental factors and inherent variability that traditional deterministic models may overlook. By incorporating stochastic elements, the model better reflects real-world complexities, such as unexpected fluctuations in disease spread due to environmental changes, social behaviors, or other unpredictable influences. This approach ensures that the model not only captures the average behavior of an epidemic but also the potential deviations from expected outcomes, providing a more comprehensive and realistic understanding of disease progression [18, 19].

The methodology we adopt in this study involves the development of novel Lyapunov functions and the construction of a rectangular set, both designed to be independent of the positive equilibrium \mathcal{E}^+ found in the deterministic counterpart of the model. This independence is crucial for accurately analyzing the stability and long-term behavior of the system under stochastic influences [20, 21].

In epidemiological studies, it is well-recognized that many infectious diseases exhibit temporal variations that often correspond with seasonal changes. These variations significantly impact the spread and intensity of epidemics, making it essential to incorporate time-periodic coefficients into the analysis of disease dynamics. The inclusion of these periodic factors aligns the model more closely with real-world scenarios, where disease incidence may rise and fall cyclically due to factors such as temperature changes, population movements, or seasonal human activities [22–24].

In this study, we work within the framework of a complete probability space, which we denote by $(\Omega, \mathcal{F}, \{\mathcal{F}_t\}_{t \geq 0}, \mathbb{P})$. This probability space is structured to include a filtration $\{\mathcal{F}_t\}_{t \geq 0}$ that satisfies the standard assumptions typically required in stochastic processes, such as being right-continuous and containing all \mathbb{P} -null sets. These conditions are essential for ensuring that the filtration appropriately models the flow of information over time, which is critical for the analysis of stochastic dynamics in the model.

Let $\mathbb{R}^+ = [0, \infty)$ be the non-negative real line, and $\mathbb{R}_+^4 = \{(\hbar_1, \hbar_2, \hbar_3, \hbar_4) \in \mathbb{R}^4 : \hbar_i > 0, i = 1, 2, 3, 4\}$ represents the positive orthant in four-dimensional space.

For an integrable function $\ell(t)$ over the interval $[0, \infty)$, we define its time-averaged value as $\langle \ell \rangle_t = \frac{1}{t} \int_0^t \ell(s) ds$. When dealing with a bounded function $\ell(t)$ defined on $[0, \infty)$, we use the notations $\hat{\ell} = \inf_{t \in [0, \infty)} \ell(t)$ and $\check{\ell} = \sup_{t \in [0, \infty)} \ell(t)$ to indicate its essential infimum and supremum, respectively.

We now present the following theorem, which establishes the existence and uniqueness of positive solutions for the proposed dynamical system.

Theorem 1.1. *Assume that the stochastic system described by Eq (1.3) has an initial condition $(\mathcal{S}_0, \mathcal{V}_0, \mathcal{I}_0, \mathcal{R}_0) \in \mathbb{R}_+^4$. Then, for all $t \geq 0$, the system admits a unique and positive solution $(\mathcal{S}_t, \mathcal{V}_t, \mathcal{I}_t, \mathcal{R}_t) \in \mathbb{R}_+^4$ almost surely.*

Moreover, the solution $(\mathcal{S}_t, \mathcal{V}_t, \mathcal{I}_t, \mathcal{R}_t)$ satisfies the following long-term properties:

$$\lim_{t \rightarrow \infty} \frac{\mathcal{S}_t}{t} = 0, \quad \lim_{t \rightarrow \infty} \frac{\mathcal{V}_t}{t} = 0, \quad \lim_{t \rightarrow \infty} \frac{\mathcal{I}_t}{t} = 0, \quad \lim_{t \rightarrow \infty} \frac{\mathcal{R}_t}{t} = 0, \quad a.s. \quad (1.4)$$

Additionally, the following upper bounds hold:

$$\limsup_{t \rightarrow \infty} \frac{\log \mathcal{S}_t}{t} \leq 0, \quad \limsup_{t \rightarrow \infty} \frac{\log \mathcal{V}_t}{t} \leq 0, \quad \limsup_{t \rightarrow \infty} \frac{\log \mathcal{I}_t}{t} \leq 0, \quad \limsup_{t \rightarrow \infty} \frac{\log \mathcal{R}_t}{t} \leq 0, \quad a.s. \quad (1.5)$$

Furthermore, if $\mu(t)$ satisfies the condition

$$\mu(t) > \frac{\sigma_1^2(t) \vee \sigma_2^2(t)}{2}, \quad (1.6)$$

then the following limits hold:

$$\lim_{t \rightarrow \infty} \frac{1}{t} \int_0^t \mathcal{S}(r) d\mathcal{B}_1(r) = 0, \quad \lim_{t \rightarrow \infty} \frac{1}{t} \int_0^t \mathcal{I}(r) d\mathcal{B}_2(r) = 0, \quad a.s. \quad (1.7)$$

The proof of Theorem (1.1) follows a methodology similar to that used in Theorem 2.1 [18] and is supported by Lemmas 2.1 and 2.2 in [25]. As the reasoning is analogous, we will not reproduce the full details of the proof here.

2. Disease extinction and long-term persistence

This section delves into the conditions that determine whether the disease \mathcal{I}_t will die out (extinction) or continue to persist over time. We begin by establishing a theorem that provides the conditions under which the disease will go extinct.

Theorem 2.1. *Let the parameter μ be such that $\mu > \max\left(\frac{\sigma_1^2}{2}, \frac{\sigma_2^2}{2}\right)$. Consider a solution $(\mathcal{S}_t, \mathcal{V}_t, \mathcal{I}_t, \mathcal{R}_t)$ to the system given by Eq (1.3), where the initial values $(\mathcal{S}_0, \mathcal{V}_0, \mathcal{I}_0, \mathcal{R}_0)$ are within the positive orthant \mathbb{R}_+^4 . Let us consider that the basic reproduction number, denoted as \mathfrak{R}_0^* , is characterized by the following expression:*

$$\mathfrak{R}_0^* := \frac{\beta\mu}{(\mu_1 + \alpha)(\mu_3 + \gamma + \omega + \frac{\sigma_2^2}{2})} + \frac{\beta_1\mu}{\mu_2(\mu_3 + \gamma + \omega + \frac{\sigma_2^2}{2})},$$

and further suppose that this quantity satisfies the condition

$$\mathfrak{R}_0^* < 1.$$

Under these assumptions, the solution $(\mathcal{S}_t, \mathcal{V}_t, \mathcal{I}_t, \mathcal{R}_t)$ satisfies the following asymptotic behavior:

$$\limsup_{t \rightarrow \infty} \frac{\log \mathcal{I}_t}{t} \leq (\mu_3 + \gamma + \omega + \frac{\sigma_2^2}{2})(\mathfrak{R}_0^* - 1) < 0, \quad \text{almost surely.}$$

This result indicates that the disease will eventually die out with probability one.

Proof. We start by analyzing the first equation in the system described by Eq (1.3). This equation gives the dynamics of the susceptible population \mathcal{S}_t . Dividing the equation by t and rearranging terms, we have

$$\frac{\mathcal{S}_t - \mathcal{S}_0}{t} = \mu - \mu_1 \langle \mathcal{S} \rangle_t - \beta \langle \mathcal{S} \mathcal{I} \rangle_t - \alpha \langle \mathcal{S} \rangle_t - \frac{\sigma_1}{t} \int_0^t \mathcal{S}(r) d\mathcal{B}_1(r).$$

Next, we solve for $\langle \mathcal{S} \rangle_t$ explicitly:

$$\mu - \mu_1 \langle \mathcal{S} \rangle_t - \alpha \langle \mathcal{S} \rangle_t - \beta \langle \mathcal{S} \mathcal{I} \rangle_t - \frac{\sigma_1}{t} \int_0^t \mathcal{S}(r) d\mathcal{B}_1(r) = \frac{\mathcal{I}_t - \mathcal{I}_0}{t}.$$

Rearranging this equation yields

$$\mu = (\mu_1 + \alpha) \langle \mathcal{S} \rangle_t + \beta \langle \mathcal{S} \mathcal{I} \rangle_t + \frac{\mathcal{I}_t - \mathcal{I}_0}{t} + \frac{\sigma_1}{t} \int_0^t \mathcal{S}(r) d\mathcal{B}_1(r).$$

Thus, solving for $\langle \mathcal{S} \rangle_t$ gives

$$\langle \mathcal{S} \rangle_t = \frac{\mu}{\mu_1 + \alpha} - \frac{\beta}{\mu_1 + \alpha} \langle \mathcal{S} \mathcal{I} \rangle_t - \delta_1(t),$$

where the term $\delta_1(t)$ is defined as

$$\delta_1(t) = \frac{1}{\mu_1 + \alpha} \left(\frac{\sigma_1}{t} \int_0^t \mathcal{S}(r) d\mathcal{B}_1(r) + \frac{\mathcal{I}_t - \mathcal{I}_0}{t} \right).$$

Utilizing the strong law of large numbers applicable to martingales, along with the fundamental characteristics of stochastic integrals, it can be established that the stochastic component converges to zero as $t \rightarrow \infty$. Therefore, we conclude that

$$\lim_{t \rightarrow \infty} \delta_1(t) = 0, \quad \text{almost surely.}$$

This leads to the following upper bound for $\langle \mathcal{S} \rangle_t$:

$$\limsup_{t \rightarrow \infty} \langle \mathcal{S} \rangle_t \leq \frac{\mu}{\mu_1 + \alpha}, \quad \text{almost surely.} \quad (2.1)$$

Next, we consider the second equation in the system described by Eq (1.3). This equation gives the dynamics of the vaccinated population \mathcal{V}_t . Dividing the equation by t and rearranging terms, we have

$$\frac{\mathcal{V}_t - \mathcal{V}_0}{t} = \alpha \langle \mathcal{S} \rangle_t - \beta_1 \langle \mathcal{V} \mathcal{I} \rangle_t - (\gamma_1 + \mu_2) \langle \mathcal{V} \rangle_t + \frac{\sigma_1}{t} \int_0^t \mathcal{S}(r) d\mathcal{B}_1(r),$$

Next, we solve for $\langle \mathcal{V} \rangle_t$ explicitly:

$$\alpha \langle \mathcal{S} \rangle_t - \beta_1 \langle \mathcal{V} \mathcal{I} \rangle_t - (\gamma_1 + \mu_2) \langle \mathcal{V} \rangle_t + \frac{\sigma_1}{t} \int_0^t \mathcal{S}(r) d\mathcal{B}_1(r) = \frac{\mathcal{V}_t - \mathcal{V}_0}{t}.$$

Rearranging this equation yields

$$(\gamma_1 + \mu_2) \langle \mathcal{V} \rangle_t = \alpha \langle \mathcal{S} \rangle_t - \beta_1 \langle \mathcal{V} \mathcal{I} \rangle_t - \frac{\mathcal{V}_t - \mathcal{V}_0}{t} + \frac{\sigma_1}{t} \int_0^t \mathcal{S}(r) d\mathcal{B}_1(r).$$

Thus, solving for $\langle \mathcal{V} \rangle_t$ gives

$$\langle \mathcal{V} \rangle_t = \frac{\alpha \langle \mathcal{S} \rangle_t}{\gamma_1 + \mu_2} - \frac{\beta_1}{\gamma_1 + \mu_2} \langle \mathcal{V} \mathcal{I} \rangle_t + \delta_2(t),$$

where the term $\delta_2(t)$ is defined as

$$\delta_2(t) = \frac{1}{\gamma_1 + \mu_2} \left(\frac{\sigma_1}{t} \int_0^t \mathcal{I}(r) d\mathcal{B}_1(r) - \frac{\mathcal{V}_t - \mathcal{V}_0}{t} \right).$$

Utilizing the strong law of large numbers applicable to martingales, along with the fundamental characteristics of stochastic integrals, it can be established that the stochastic component converges to zero as $t \rightarrow \infty$. Therefore, we conclude that

$$\lim_{t \rightarrow \infty} \delta_2(t) = 0, \quad \text{almost surely.}$$

This leads to the following upper bound for $\langle \mathcal{V} \rangle_t$:

$$\langle \mathcal{V} \rangle_t = \frac{\alpha \langle \mathcal{I} \rangle_t}{\gamma_1 + \mu_2} - \frac{\beta_1}{\gamma_1 + \mu_2} \langle \mathcal{V} \mathcal{I} \rangle_t.$$

From (2.1), one can get

$$\limsup_{t \rightarrow \infty} \langle \mathcal{V} \rangle_t \leq \frac{\alpha \mu}{(\gamma_1 + \mu_2)(\mu_1 + \alpha)}, \quad \text{almost surely.} \quad (2.2)$$

Now, considering the entire system in (1.3), we sum up the differential equations to get the total population equation:

$$\frac{\mathcal{R}_t - \mathcal{R}_0}{t} + \frac{\mathcal{I}_t - \mathcal{I}_0}{t} + \frac{\mathcal{V}_t - \mathcal{V}_0}{t} + \frac{\mathcal{S}_t - \mathcal{S}_0}{t} = \mu - \mu_1 \langle \mathcal{I} \rangle_t - \mu_2 \langle \mathcal{V} \rangle_t - (\mu_3 + \omega) \langle \mathcal{I} \rangle_t - \mu_4 \langle \mathcal{R} \rangle_t.$$

This equation can be rearranged as

$$\mu_1 \langle \mathcal{I} \rangle_t + \mu_2 \langle \mathcal{V} \rangle_t + (\mu_3 + \omega) \langle \mathcal{I} \rangle_t + \mu_4 \langle \mathcal{R} \rangle_t = \mu. \quad (2.3)$$

Next, we apply Ito's lemma to the third equation of the system (1.3), which governs the dynamics of the infected population \mathcal{I}_t . This yields

$$\frac{\log \mathcal{I}_t - \log \mathcal{I}_0}{t} = \beta \langle \mathcal{I} \rangle_t + \beta_1 \langle \mathcal{V} \rangle_t - \mu_3 - \gamma - \omega - \frac{\sigma_2^2}{2} + \frac{\sigma_2 \mathcal{B}_2(t)}{t}.$$

By inserting the expression for $\langle \mathcal{V} \rangle_t$, provided in Eq (2.3) into the current equation, we obtain the following result:

$$\begin{aligned} \frac{\log \mathcal{I}_t - \log \mathcal{I}_0}{t} &= \left(\beta - \frac{\beta_1 \mu_1}{\mu_2} \right) \langle \mathcal{I} \rangle_t + \frac{\beta_1 \mu}{\mu_2} - (\mu_3 + \gamma + \omega + \frac{\sigma_2^2}{2}) \\ &\quad - \frac{\beta_1 (\mu_3 + \gamma)}{\mu_2} \langle \mathcal{I} \rangle_t - \frac{\beta_1 \mu_4}{\mu_2} \langle \mathcal{R} \rangle_t + \delta_3(t), \\ &\leq \frac{\beta \mu}{\mu_1 + \alpha} + \frac{\beta_1 \mu}{\mu_2} - (\mu_3 + \gamma + \omega + \frac{\sigma_2^2}{2}) - \frac{\beta_1 \mu_1}{\mu_2} \langle \mathcal{I} \rangle_t \\ &\quad - \frac{\beta_1 (\mu_3 + \gamma)}{\mu_2} \langle \mathcal{I} \rangle_t - \frac{\beta_1 \mu_4}{\mu_2} \langle \mathcal{R} \rangle_t + \delta_3(t), \end{aligned} \quad (2.4)$$

where $\delta_3(t)$ is a term that converges to zero almost surely as $t \rightarrow \infty$.

Taking the limit superior of both sides of Eq (2.4), and combining the results from (2.1) and (2.3), we obtain

$$\limsup_{t \rightarrow \infty} \frac{\log \mathcal{I}_t}{t} \leq \left(\mu_3 + \gamma + \omega + \frac{\sigma_2^2}{2} \right) (\mathfrak{R}_0^* - 1), \quad \text{almost surely.}$$

Therefore, if $\mathfrak{R}_0^* < 1$, then $\lim_{t \rightarrow \infty} \mathcal{I}_t = 0$, almost surely, indicating that the disease will become extinct with probability one. \square

Theorem 2.2. *If*

$$\begin{aligned} \mathfrak{R}_0^* = & \frac{\beta\mu}{(\mu + \alpha + \sigma_1^2/2)(\gamma + \mu_3 + \omega + \sigma_2^2/2)} \\ & + \frac{\beta_1\mu\alpha}{(\mu + \alpha + \sigma_1^2/2)(\mu_2 + \gamma_1 + \sigma_1^2/2)(\gamma + \mu_3 + \omega + \sigma_2^2/2)} > 1, \end{aligned}$$

then for any initial value $(\mathcal{S}_0, \mathcal{V}_0, \mathcal{I}_0, \mathcal{R}_0) \in \mathbb{R}_+^4$, the infected population \mathcal{I}_t of the model has the property

$$\liminf_{t \rightarrow \infty} \langle \mathcal{I} \rangle_t \geq \frac{(\gamma + \mu_3 + \omega + \sigma_2^2/2)(\mathfrak{R}_0^* - 1)}{(a_1 + b_1)\beta + b_2\beta_1}, \quad \text{a.s.},$$

where

$$a_1 = \frac{\beta\mu}{\mu + \alpha + \sigma_1^2/2}, \quad b_1 = \frac{\beta_1\mu\alpha}{(\mu + \alpha + \sigma_1^2/2)(\mu_2 + \gamma_1 + \sigma_1^2/2)}, \quad b_2 = \frac{\beta_1\mu\alpha}{(\mu + \alpha + \sigma_1^2/2)(\mu_2 + \gamma_1 + \sigma_1^2/2)}.$$

In other words, this result indicates that the disease will continue to spread and persist in the population if the basic reproduction number \mathfrak{R}_0^* exceeds the critical threshold of 1. Specifically, when $\mathfrak{R}_0^* > 1$, each infected individual, on average, generates more than one new infection, which leads to sustained transmission and the continued presence of the disease within the population.

Proof. Set

$$\mathfrak{B}(\mathcal{S}, \mathcal{V}, \mathcal{I}, \mathcal{R}) = -\log \mathcal{I} - (a_1 + b_1) \log \mathcal{S} - b_2 \log \mathcal{V} - c_1 \log \mathcal{R},$$

where positive constants a_1 , b_1 , b_2 , and c_1 will be established in subsequent calculations. By utilizing Ito's lemma, we derive the following result.

$$d\mathfrak{B} = \mathfrak{B} dt - (a_1 + b_1)\sigma_1 d\mathcal{B}_1(t) - b_2\sigma_1 d\mathcal{B}_1(t) - c_1\sigma_2 d\mathcal{B}_2(t) - \sigma_2 d\mathcal{B}_2(t), \quad (2.5)$$

where

$$\begin{aligned}
 \mathcal{L}\mathfrak{B} &= \mathcal{L}(-\log \mathcal{I} - (a_1 + b_1) \log \mathcal{S} - b_2 \log \mathcal{V} - c_1 \log \mathcal{R}) \\
 &= -\beta \mathcal{S} - \beta_1 \mathcal{V} + \gamma + \mu_3 + \omega + \frac{\sigma_2^2}{2} \\
 &\quad - \frac{a_1 \mu}{\mathcal{S}} + a_1 \left(\mu + \alpha + \frac{\sigma_1^2}{2} \right) + a_1 \beta \mathcal{S} \\
 &\quad - \frac{b_1 \mu}{\mathcal{S}} + b_1 \left(\mu + \alpha + \frac{\sigma_1^2}{2} \right) + b_1 \beta \mathcal{S} \\
 &\quad - \frac{b_2 \alpha \mathcal{S}}{\mathcal{V}} + b_2 \beta_1 \mathcal{S} + b_2 \left(\mu_2 + \gamma_1 + \frac{\sigma_1^2}{2} \right) \\
 &\quad - \frac{c_1 \mu_4}{\mathcal{R}} + c_1 \gamma_1 + c_1 \gamma + c_1 \frac{\sigma_2^2}{2} + \gamma + \mu_3 + \omega + \frac{\sigma_2^2}{2} + ((a_1 + b_1)\beta + b_2 \beta_1) \mathcal{S}.
 \end{aligned}$$

Let

$$\begin{aligned}
 a_1 &= \frac{\beta \mu}{\mu + \alpha + \sigma_1^2/2}, \\
 b_1 &= \frac{\beta_1 \mu \alpha}{(\mu + \alpha + \sigma_1^2/2)(\mu_2 + \gamma_1 + \sigma_1^2/2)}, \\
 b_2 &= \frac{\beta_1 \mu \alpha}{(\mu + \alpha + \sigma_1^2/2)(\mu_2 + \gamma_1 + \sigma_1^2/2)}, \\
 c_1 &= \frac{\gamma + \mu_3 + \omega + \sigma_2^2/2}{\gamma_1}.
 \end{aligned}$$

Then

$$\begin{aligned}
 \mathcal{L}\mathfrak{B} &\leq -\frac{\beta \mu}{\mu + \alpha + \sigma_1^2/2} - \frac{\beta_1 \mu \alpha}{(\mu + \alpha + \sigma_1^2/2)(\mu_2 + \gamma_1 + \sigma_1^2/2)} + \gamma + \mu_3 + \omega + \frac{\sigma_2^2}{2} \\
 &\quad + ((a_1 + b_1)\beta + b_2 \beta_1) \mathcal{S}.
 \end{aligned} \tag{2.6}$$

This simplifies to

$$\mathcal{L}\mathfrak{B} \leq -(\gamma + \mu_3 + \omega + \frac{\sigma_2^2}{2})(\mathfrak{R}_0^* - 1) + ((a_1 + b_1)\beta + b_2 \beta_1) \mathcal{S}. \tag{2.7}$$

By replacing the expression given in Eq (2.7) into Eq (2.5), and then performing integration on both sides of Eq (2.5), we derive the following outcome:

$$\begin{aligned}
 \frac{1}{t} [\mathfrak{B}(\mathcal{I}_t, \mathcal{V}_t, \mathcal{I}_t, \mathcal{R}_t) - \mathfrak{B}(\mathcal{I}_0, \mathcal{V}_0, \mathcal{I}_0, \mathcal{R}_0)] &\leq -\left(\gamma + \mu_3 + \omega + \frac{\sigma_2^2}{2} \right) (\mathfrak{R}_0^* - 1) \\
 &\quad + [(a_1 + b_1)\beta + b_2 \beta_1] \langle \mathcal{I} \rangle_t - \frac{\mathcal{M}(t)}{t},
 \end{aligned} \tag{2.8}$$

where $\mathcal{M}(t)$ is a martingale given by

$$\mathcal{M}(t) = (a_1 + b_1) \int_0^t \sigma_1 d\mathcal{B}_1(s) + b_2 \int_0^t \sigma_1 d\mathcal{B}_1(s) + c_1 \int_0^t \sigma_2 d\mathcal{B}_2(s) + \int_0^t \sigma_2 d\mathcal{B}_2(s).$$

Applying the strong law of large numbers for martingales, we can deduce that as t approaches infinity, the expression

$$\lim_{t \rightarrow \infty} \frac{\mathcal{M}(t)}{t} = 0, \quad \text{a.s.}$$

converges to zero. This implies that the contribution of the martingale term becomes negligible in the long run.

$$\liminf_{t \rightarrow \infty} \frac{1}{t} [\mathfrak{B}(\mathcal{I}_t, \mathcal{V}_t, \mathcal{I}_t, \mathcal{R}_t) - \mathfrak{B}(\mathcal{I}_0, \mathcal{V}_0, \mathcal{I}_0, \mathcal{R}_0)] \leq \liminf_{t \rightarrow \infty} \left[- \left(\gamma + \mu_3 + \omega + \frac{\sigma_2^2}{2} \right) (\mathfrak{R}_0^* - 1) + [(a_1 + b_1)\beta + b_2\beta_1] \langle \mathcal{I} \rangle_t \right].$$

As t grows indefinitely, the difference term $\frac{1}{t} [\mathfrak{B}(\mathcal{I}_t, \mathcal{V}_t, \mathcal{I}_t, \mathcal{R}_t) - \mathfrak{B}(\mathcal{I}_0, \mathcal{V}_0, \mathcal{I}_0, \mathcal{R}_0)]$ gradually diminishes. This is due to the application of the strong law of large numbers for martingales, which guarantees that the limit of this difference as t tends to infinity is zero almost surely. Therefore, we can assert:

$$\lim_{t \rightarrow \infty} \frac{1}{t} [\mathfrak{B}(\mathcal{R}_t, \mathcal{I}_t, \mathcal{V}_t, \mathcal{I}_t) - \mathfrak{B}(\mathcal{R}_0, \mathcal{I}_0, \mathcal{V}_0, \mathcal{I}_0)] = 0.$$

Given this result, it follows directly that:

$$\liminf_{t \rightarrow \infty} \frac{1}{t} [\mathfrak{B}(\mathcal{R}_t, \mathcal{I}_t, \mathcal{V}_t, \mathcal{I}_t) - \mathfrak{B}(\mathcal{R}_0, \mathcal{I}_0, \mathcal{V}_0, \mathcal{I}_0)] = 0.$$

Therefore, the inequality simplifies to:

$$0 \leq - \left(\gamma + \mu_3 + \omega + \frac{\sigma_2^2}{2} \right) (\mathfrak{R}_0^* - 1) + [(a_1 + b_1)\beta + b_2\beta_1] \liminf_{t \rightarrow \infty} \langle \mathcal{I} \rangle_t.$$

Furthermore,

$$\liminf_{t \rightarrow \infty} \langle \mathcal{I} \rangle_t \geq \frac{(\gamma + \mu_3 + \omega + \frac{\sigma_2^2}{2})(\mathfrak{R}_0^* - 1)}{(a_1 + b_1)\beta + b_2\beta_1}.$$

This completes the proof. \square

2.1. Remark

The deterministic reproduction number and the stochastic threshold values are connected, as stochastic perturbations modify the effective threshold. High stochastic intensities can drive disease extinction by destabilizing infection dynamics. Stochastic perturbations introduce variability, altering disease persistence and extinction probabilities. These insights highlight the need for stochastic modeling in realistic epidemic predictions. The deterministic model uses a basic reproduction number to determine disease persistence. In the stochastic model, this threshold is modified due to the presence of random perturbations. Stochastic fluctuations lower the effective reproduction number, making disease extinction more likely even when the deterministic model predicts persistence. Stronger stochastic fluctuations increase the probability of disease extinction. When random noise intensity reaches a certain level, it disrupts transmission dynamics enough to drive the infection out of the population. This highlights how real-world uncertainties, such as environmental or behavioral changes, can influence disease spread and control. These findings emphasize the importance of incorporating stochasticity into epidemic models to better reflect real-world uncertainties and improve disease prediction and control strategies.

3. Numerical schemes and evaluation of computational results

After completing the examination of disease eradication and long-term persistence, we shift our focus to performing numerical simulations. We will execute simulations based on the model described in Eq (1.3) to illustrate the practical implications of our findings. For this purpose, we will use the following parameter values: $\mu = 0.03$, $\mu_1 = 0.04$, $\mu_2 = 0.035$, $\mu_3 = 0.06$, $\mu_4 = 0.045$, $\beta = 0.5$, $\beta_1 = 0.05$, $\gamma = 0.1$, $\gamma_1 = 0.1$, $\alpha = 0.2$, and $\omega = 0.1$. The initial conditions for the simulation are set as follows: $\mathcal{S}(0) = 0.5$, $\mathcal{V}(0) = 0.3$, $\mathcal{I}(0) = 0.2$, and $\mathcal{R}(0) = 0$. For the numerical simulations, we employ the technique of Higham [26]. Let us consider the discretized equation of the model in which ξ is a normally distributed random variable that introduces randomness into the numerical scheme and Δt is the time step controlling how frequently the system updates, which is chosen very small, equals to 0.01 or 0.001.

$$\begin{aligned}
 \mathcal{S}_{k+1} &= \mathcal{S}_k + (\mu - \mu_1 \mathcal{S}_k - \beta \mathcal{S}_k \mathcal{I}_k - \alpha \mathcal{S}_k) \Delta t - \sigma_1 \mathcal{S}_k \sqrt{\Delta t} \xi_k - \frac{1}{2} \sigma_1^2 \mathcal{S}_k (\Delta t \xi_k^2 - \Delta t), \\
 \mathcal{V}_{k+1} &= \mathcal{V}_k + (\alpha \mathcal{S}_k - \beta_1 \mathcal{V}_k \mathcal{I}_k - \gamma_1 \mathcal{V}_k - \mu_2 \mathcal{V}_k) \Delta t + \sigma_1 \mathcal{S}_k \sqrt{\Delta t} \xi_k + \frac{1}{2} \sigma_1^2 \mathcal{S}_k (\Delta t \xi_k^2 - \Delta t), \\
 \mathcal{I}_{k+1} &= \mathcal{I}_k + (\beta \mathcal{S}_k \mathcal{I}_k + \beta_1 \mathcal{V}_k \mathcal{I}_k - \gamma \mathcal{I}_k - \mu_3 \mathcal{I}_k - \omega \mathcal{I}_k) \Delta t - \sigma_2 \mathcal{I}_k \sqrt{\Delta t} \zeta_k - \frac{1}{2} \sigma_2^2 \mathcal{I}_k (\Delta t \zeta_k^2 - \Delta t), \\
 \mathcal{R}_{k+1} &= \mathcal{R}_k + (\gamma_1 \mathcal{V}_k + \gamma \mathcal{I}_k - \mu_4 \mathcal{R}_k) \Delta t + \sigma_2 \mathcal{I}_k \sqrt{\Delta t} \zeta_k + \frac{1}{2} \sigma_2^2 \mathcal{I}_k (\Delta t \zeta_k^2 - \Delta t).
 \end{aligned} \tag{3.1}$$

Following the incorporation of white noise into the system (1.3), we analyze the behavior of the susceptible class, denoted as \mathcal{S} in Figure 1. The addition of stochastic perturbations introduces randomness into the dynamics of the susceptible population, causing fluctuations that deviate from the deterministic model. The stochastic differential equation governing the \mathcal{S} class can be expressed as a modified version of the original system, incorporating a noise term. This term reflects the inherent unpredictability in the transmission dynamics due to various external factors, leading to a more realistic representation of the system under study. The resulting model provides valuable insights into the potential variability and uncertainty in the population dynamics, emphasizing the importance of accounting for random effects in epidemiological modeling.

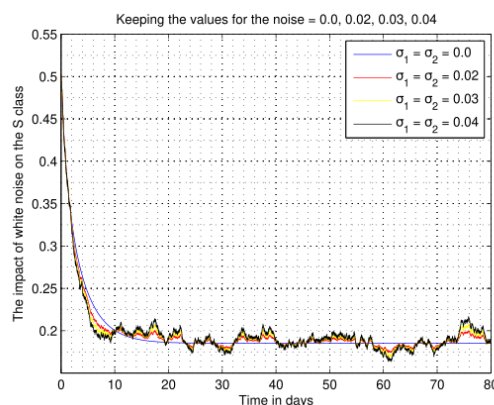


Figure 1. The path $\mathcal{S}_{(t)}$ for the model (1.3) at $\sigma_1 = \sigma_2 = 0.00, 0.02, 0.03, 0.04$.

When white noise is introduced into the system (1.3), the dynamics of the vaccinated class, denoted

by \mathcal{V} , experience stochastic fluctuations in Figure 2. The incorporation of this noise term into the differential equation for \mathcal{V} adds a layer of randomness to the vaccination process, simulating real-world uncertainties such as variability in vaccine efficacy or coverage. This stochastic perturbation causes the size of the vaccinated population to fluctuate around its deterministic path, reflecting possible variations in the rate at which individuals are vaccinated or the effectiveness of the vaccine over time. The modified model for \mathcal{V} thus captures the inherent unpredictability in the vaccination dynamics, providing a more nuanced understanding of how random factors might influence the overall success of a vaccination program.

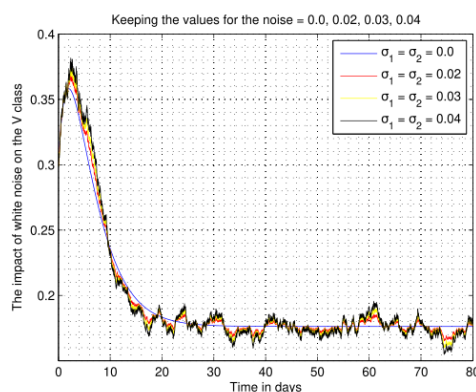


Figure 2. The path $\mathcal{V}_{(t)}$ for the model (1.3) at $\sigma_1 = \sigma_2 = 0.00, 0.02, 0.03, 0.04$.

The inclusion of white noise into the model significantly impacts the infected class, denoted by \mathcal{I} . The stochastic term introduces random fluctuations into the infection dynamics, which can represent various sources of uncertainty such as changes in contact rates, transmission variability, or other external factors affecting the spread of the disease. These random perturbations cause the number of infected individuals to deviate from the deterministic trajectory, capturing the unpredictable nature of disease transmission in a real-world setting. As a result, the modified differential equation for the infected class \mathcal{I} not only accounts for the expected progression of the disease but also reflects the possible short-term increases or decreases in the number of infected individuals due to random influences. This stochastic approach provides a more realistic portrayal of the infection dynamics, emphasizing the role of randomness in disease spread and control in Figure 3.

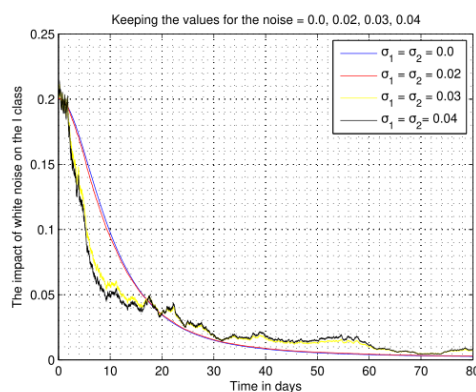


Figure 3. The path $\mathcal{I}_{(t)}$ for the model (1.3) at $\sigma_1 = \sigma_2 = 0.00, 0.02, 0.03, 0.04$.

The recovered class, denoted by \mathcal{R} , is influenced by the introduction of white noise in a manner that reflects the uncertainties associated with recovery rates. The stochastic perturbations in the model account for the randomness in the recovery process, which could stem from factors such as varying immune responses among individuals, differences in treatment efficacy, or external influences that affect recovery times. As a result, the number of recovered individuals \mathcal{R} fluctuates around its expected value, capturing the inherent variability in the recovery process in Figure 4. This addition of white noise ensures that the model more accurately represents the unpredictable nature of recovery, providing a more comprehensive understanding of how recovered individuals contribute to the overall disease dynamics in a stochastic environment.

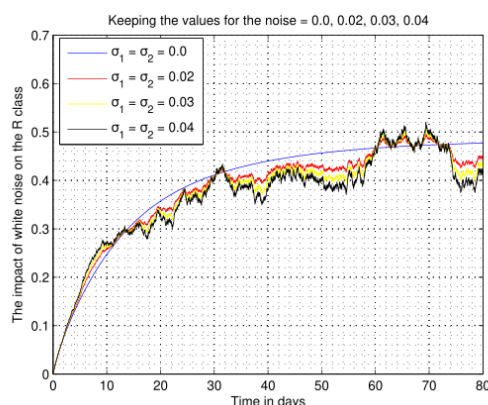


Figure 4. The path $\mathcal{R}(t)$ for the model (1.3) at $\sigma_1 = \sigma_2 = 0.00, 0.01, 0.02, 0.03$.

4. Discussion and justification

In classical epidemic modeling, deterministic approaches provide insights into disease dynamics but fail to account for real-world randomness. Our study transitions from a deterministic $\mathcal{S}\mathcal{V}\mathcal{I}\mathcal{R}$ model to a stochastic framework by introducing environmental white noise into the transmission and vaccination rates, leading to system (1.3). These stochastic perturbations capture unpredictable fluctuations in infection spread, vaccination uptake, and recovery rates, making the model more biologically realistic than its deterministic counterpart.

From the theoretical results, we establish the stochastic reproduction number \mathcal{R}_0^* . Unlike the deterministic threshold, stochastic effects introduce an additional extinction condition, meaning that even when $\mathcal{R}_0^* > 1$, random fluctuations may drive the disease to extinction. Numerical simulations confirm that increasing noise intensity (σ_1, σ_2) can lower \mathcal{R}_0^* below 1, altering long-term epidemic outcomes. This effect is absent in deterministic models, where $\mathcal{R}_0 > 1$ always predicts persistence.

Our findings align with Rozhnova and Nunes [8], who observed that randomness increases infection peak variability, emphasizing the importance of adaptive vaccination. Similarly, Gray et al [7] reported noise-induced disease resurgence, supporting our results.

The implications of these findings are substantial for public health policies. Unlike deterministic models, stochastic simulations show that small fluctuations in transmission or vaccination rates can significantly alter epidemic outcomes. These results reinforce the need for adaptive epidemic control measures, particularly in dynamic environments where real-time responses to disease fluctuations are essential.

One limitation of this model is that it assumes constant rates, whereas real-world epidemiological parameters fluctuate over time. Future research should integrate time-dependent transmission and vaccination rates, spatial effects, and real epidemiological data validation. Further exploration of stochastic control measures, such as adaptive vaccination and quarantine policies, could refine epidemic management strategies.

Overall, this study demonstrates that stochastic $SVIR$ models provide a more realistic representation of epidemic behavior than deterministic models. The stochastic framework captures randomness in disease spread, reinforcing the necessity of integrating uncertainty into epidemic modeling for better forecasting and intervention planning.

5. Conclusions

This study investigates the dynamics of disease transmission under the influence of stochastic perturbations, providing a comprehensive analysis of the system's behavior. By incorporating white noise into the $SVIR$ model, we have effectively captured the inherent uncertainties present in real-world scenarios, particularly in infection, recovery, and vaccination processes. The stochastic model not only aligns more closely with observed epidemiological data but also offers deeper insights into the conditions for disease persistence and extinction. Our findings highlight the critical role of randomness in epidemiological models, demonstrating its significant impact on disease dynamics and predictive outcomes. This work contributes valuable insights into the complex interplay between deterministic and stochastic factors in epidemic modeling, offering a robust framework for future research and public health strategies aimed at controlling infectious diseases. The implications of this study are broad, paving the way for refinements in epidemiological modeling and improved disease management practices.

Author's contributions

Shah Hussain: Writing original draft, software, methodology, formal analysis; Naveed Iqbal: Writing review and editing, visualization, validation, supervision; Elissa Nadia Madi: Investigation, formal analysis, conceptualization; Mohsen Bakouri: Visualization, validation, supervision; Ilyas Khan: Methodology, analysis, writing review and editing, supervision; Wei Sin Koh: Investigation, formal analysis, conceptualization.

All authors have agreed to and given their consent for the publication of this research paper.

Use of Generative-AI tools declaration

All authors declare that no Artificial Intelligence (AI) tools were used in the creation of this article.

Acknowledgments

The author Mohsen Bakouri extends his appreciation to the Deanship of Postgraduate Studies and Scientific Research at Majmaah University for funding this research work through the project number (R-2025-1590).

Conflict of interest

All authors declare no conflicts of interest in this paper.

References

1. A. Alkhazzan, J. Wang, Y. Nie, H. Khan, J. Alzabut, A stochastic Susceptible Vaccines Infected Recovered epidemic model with three types of noises, *Math. Method. Appl. Sci.*, **47** (2024), 8748–8770. <https://doi.org/10.1002/mma.10042>
2. A. Alkhazzan, J. Wang, Y. Nie, H. Khan, J. Alzabut, An effective transport-related SVIR stochastic epidemic model with media coverage and Lévy noise, *Chaos Soliton. Fract.*, **175** (2023), 113953. <https://doi.org/10.1016/j.chaos.2023.113953>
3. A. Alkhazzan, J. Wang, Y. Nie, K. Hattaf, A new stochastic split-step θ -nonstandard finite difference method for the developed SVIR epidemic model with temporary immunities and general incidence rates, *Vaccines*, **10** (2022), 1682. <https://doi.org/10.3390/vaccines10101682>
4. H. J. Alsakaji, F. A. Rihan, A. Hashish, Dynamics of a stochastic epidemic model with vaccination and multiple time-delays for COVID-19 in the UAE, *Complexity*, **2022** (2022), 4247800. <https://doi.org/10.1155/2022/4247800>
5. L. J. S. Allen, A primer on stochastic epidemic models: Formulation, numerical simulation, and analysis, *Infectious Disease Modelling*, **2** (2017), 128–142. <https://doi.org/10.1016/j.idm.2017.03.001>
6. F. Brauer, Backward bifurcations in simple vaccination/treatment models, *J. Biol. Dynam.*, **5** (2011), 410–418. <https://doi.org/10.1080/17513758.2010.510584>
7. A. Gray, D. Greenhalgh, L. Hu, X. Mao, J. Pan, A stochastic differential equation SIS epidemic model, *SIAM J. Appl. Math.*, **71** (2011), 876–902. <https://doi.org/10.1137/10081856X>
8. G. Rozhnova, A. Nunes, Stochastic effects in a seasonally forced epidemic model, *Phys. Rev. E.*, **82** (2010), 041906. <https://doi.org/10.1103/PhysRevE.82.041906>
9. P. J. Witbooi, Stability of a stochastic model of an SIR epidemic with vaccination, *Acta Biotheor.*, **65** (2017), 151–165. <https://doi.org/10.1007/s10441-017-9308-5>
10. J. Harianto, T. Suparwati, SVIR epidemic model with non constant population, *CAUCHY-Jurnal Matematika Murni dan Aplikasi*, **5** (2018), 102–111. <https://doi.org/10.18860/ca.v5i3.5511>
11. Y. Cai, Y. Kang, M. Banerjee, W. Wang, A stochastic epidemic model incorporating media coverage, *Commun. Math. Sci.*, **14** (2016), 893–910. <https://doi.org/10.4310/CMS.2016.v14.n4.a1>
12. M. Liu, M. Fan, Permanence of stochastic Lotka-Volterra systems, *J. Nonlinear Sci.*, **27** (2017), 425–452. <https://doi.org/10.1007/s00332-016-9337-2>
13. W. Wang, Y. Cai, Z. Ding, Z. Gui, A stochastic differential equation SIS epidemic model incorporating Ornstein–Uhlenbeck process, *Physica A*, **509** (2018), 921–936. <https://doi.org/10.1016/j.physa.2018.06.099>
14. A. Lahrouz, L. Omari, Extinction and stationary distribution of a stochastic SIRS epidemic model with non-linear incidence, *Stat. Probabil. Lett.*, **83** (2013), 960–968. <https://doi.org/10.1016/j.spl.2012.12.021>

15. X. Zhang, K. Wang, Stochastic model for spread of AIDS driven by Lévy noise, *J. Dyn. Diff. Equat.*, **27** (2015), 215–236. <https://doi.org/10.1007/s10884-015-9459-5>
16. Y. Zhao, D. Jiang, The threshold of a stochastic SIS epidemic model with vaccination, *Appl. Math. Comput.*, **243** (2014), 718–727. <https://doi.org/10.1016/j.amc.2014.05.124>
17. Q. Yang, D. Jiang, N. Shi, C. Ji, The ergodicity and extinction of stochastically perturbed SIR and SEIR epidemic models with saturated incidence, *J. Math. Anal. Appl.*, **388** (2012), 248–271. <https://doi.org/10.1016/j.jmaa.2011.11.072>
18. C. Ji, D. Jiang, Q. Yang, N. Shi, Dynamics of a multigroup SIR epidemic model with stochastic perturbation, *Automatica*, **48** (2012), 121–131. <https://doi.org/10.1016/j.automatica.2011.09.044>
19. D. Jiang, J. Yu, C. Ji, N. Shi, Asymptotic behavior of global positive solution to a stochastic SIR model, *Math. Comput. Model.*, **54** (2011), 221–232. <https://doi.org/10.1016/j.mcm.2011.02.004>
20. R. Rudnicki, Long-time behavior of a stochastic prey–predator model, *Stoch. Proc. Appl.*, **108** (2003), 93–107. [https://doi.org/10.1016/S0304-4149\(03\)00090-5](https://doi.org/10.1016/S0304-4149(03)00090-5)
21. F. A. Rihan, H. J. Alsakaji, Dynamics of a stochastic delay differential model for COVID-19 infection with asymptomatic infected and interacting people: Case study in the UAE, *Results Phys.*, **28** (2021), 104658. <https://doi.org/10.1016/j.rinp.2021.104658>
22. Y. Lin, D. Jiang, T. Liu, Nontrivial periodic solution of a stochastic epidemic model with seasonal variation, *Appl. Math. Lett.*, **45** (2015), 103–107. <https://doi.org/10.1016/j.aml.2015.01.021>
23. X. Zhang, D. Jiang, A. Alsaedi, T. Hayat, Periodic solutions and stationary distribution of mutualism models in random environments, *Physica A*, **460** (2016), 270–282. <https://doi.org/10.1016/j.physa.2016.05.015>
24. Y. Zhao, D. Jiang, The threshold of a stochastic SIS epidemic model with vaccination, *Appl. Math. Comput.*, **243** (2014), 718–727. <https://doi.org/10.1016/j.amc.2014.05.124>
25. C. Zhu, G. Yin, Asymptotic properties of hybrid diffusion systems, *SIAM J. Control Optim.*, **46** (2007), 1155–1179. <https://doi.org/10.1137/060649343>
26. D. J. Higham, An algorithmic introduction to numerical simulation of stochastic differential equations, *SIAM Rev.*, **43** (2001), 525–546. <https://doi.org/10.1137/S0036144500378302>



AIMS Press

© 2025 the Author(s), licensee AIMS Press. This is an open access article distributed under the terms of the Creative Commons Attribution License (<https://creativecommons.org/licenses/by/4.0>)